Green Chemistry

PAPER

Cite this: *Green Chem.*, 2019, **21**, 6407

An integrated process combining the reaction and purification of PEGylated proteins†

João H. P. M. Santos,[a,b] Carlos M. N. Mendonça,[a,b] Amanda R. P. Silva,[a] Ricardo P. S. Oliveira,[a] Adalberto Pessoa, Jr,[a] João A. P. Coutinho,[b] Sónia P. M. Ventura[b] and Carlota O. Rangel-Yagui *[a]

A downstream process combining PEGylation reaction and the use of enzyme conjugates acting as phase-forming components of aqueous biphasic systems (ABS) is proposed here. In this approach, citrate buffer (pH = 7.0) was used simultaneously to stop the reaction (avoiding the use of hydroxylamine) and as a phase forming agent inducing the phase separation of the PEGylated proteins. The partition of the bioconjugates was assessed using two model enzymes of small size [cytochrome c (Cyt-c) and lysozyme (LYS)], and two of large size [L-asparaginase (ASNase) and catalase (CAT)] as well as reactive PEG of 5, 10, 20 and 40 kDa. The effect of the reaction time on the PEGylation and recovery steps was also evaluated. All reactive PEGs allowed high selectivity in the separation of PEGylated proteins from native proteins (S > 100). A positive effect in terms of selectivity was found for longer reaction times. It allowed greater amounts of PEGylated proteins, with an increase of the PEG-protein rich-phase volume (top phase), allowing 100% of recovery of PEGylated proteins. More selective systems were obtained for Cyt-c and LYS (S > 100) compared to those for ASNase and CAT (40 < S < 60); nevertheless for all, the native and PEGylated proteins had their biological activity preserved. Envisioning the industrial potential evaluation, an integrated process diagram was defined combining the PEGylation reaction with the purification of the protein conjugates. Two different scenarios were investigated considering the PEGylation reaction performance. For both approaches (complete and incomplete PEGylation reaction), high recovery yields and purities were achieved for the PEGylated conjugates (92.1 ± 0.4% < $\%RecT_{Cyt\text{-}c\text{-}PEG}$ < 98.1 ± 0.1%; 84.6% < purity < 100%) and for the unreacted enzyme ($\%RecB_{Cyt\text{-}c}$ = 81 ± 1%; purity = 97.7%), while maintaining their structural integrity.

Received 3rd May 2019,
Accepted 18th October 2019

DOI: 10.1039/c9gc01459d

rsc.li/greenchem

Introduction

Therapeutic biological products based on proteins and peptides are of increasing interest in the pharmaceutical field.[1,2] This class of drugs is characterized by its high specificity, offering the possibility to treat complex diseases once considered untreatable. Nonetheless, protein drugs are usually associated with low solubility profiles, short shelf-lives, short circulating half-lives and susceptibility to cleavage by proteolytic enzymes.[2,3] To date, several techniques have been implemented to increase solubility, improve molecular stabilization and enhance protein pharmacokinetics.[4–6] Most of these techniques focus on the bioconjugation of proteins with polymers, generating improved drugs, *i.e.* biobetters, which are superior when compared to the original biological.[7,8] Among the large array of bioconjugation techniques, PEGylation is the most favorable alternative. This strategy is FDA and EMA approved and it has been used in the development of several protein drugs currently on the market.[7–9] Through careful selection of the reaction chemistry, one or more polyethylene glycol (PEG) molecules can be attached to the proteins, producing PEG–protein conjugated species with one or more grafted polymeric chains.[10–13]

The biological stability and activity of PEGylated proteins are influenced by the chemical reaction used. Usually, PEGylation results in a complex mixture of proteins with varying numbers of PEG chains attached to amino acid residues, which can also vary on the location at the protein surface. A small number of site-specific modifications is available, such as N-terminal PEGylation and cysteine PEGylation.

[a]*Department of Biochemical and Pharmaceutical Technology, São Paulo University, Av. Prof. Lineu Prestes n 580 Bloco 16, 05508-000 São Paulo, SP, Brazil. E-mail: corangel@usp.com.br*

[b]*CICECO – Aveiro Institute of Materials, Department of Chemistry, University of Aveiro, 3810-193 Aveiro, Portugal*

†Electronic supplementary information (ESI) available: Detailed data for the phase diagrams are presented and SDS-PAGE results and chromatograms reflecting the product distribution in both aqueous phases. See DOI: 10.1039/c9gc01459d

Nonetheless, even site specific reactions still present some degree of polydispersity.[9,12] The separation, sub-fractionation and recovery of the target PEGamer among the different PEG–protein conjugated species are crucial steps in the PEGylation process.[14] Nonetheless, still today several proteins commercialized in the PEGylated form refer to random PEGylation and the separation of PEGylated proteins from the non-PEGylated proteins is still a challenge.

Aqueous biphasic systems (ABS) are simpler alternatives to conventional organic–water solvent extraction systems, standing out not only for the separation of the PEGylated proteins from the reaction products,[15] but also for their sub-fractionation according to the number of grafted chains among the conjugates produced.[16–18] ABS are formed when either two polymers, one polymer and one kosmotropic salt, or two salts (one chaotropic salt and the other a kosmotropic salt) are mixed at appropriate concentrations.[19] The two phases are mostly composed of water and non-volatile components, thus eliminating volatile organic compounds. They have been used for a plethora of purifications in the biotechnological field, due to their mild and non-denaturing character.[20,21] The technical and economic advantages offered by ABS, such as an increase of protein recovery yields, a decrease of the processing time, scale-up feasibility and the absence of specialized equipment or highly trained personnel further support the hypothesis of an industrial substitution of chromatography-based downstream processes with ABS platforms.[22–24]

Despite the promising potential of ABS to separate PEGylated proteins, challenges such as the recycling of phase-forming components and recovery of the target biological derivatives have been pointed out as main limitations. Thus, novel insights into the development of innovative strategies to increase the industrial potential of ABS in PEGylation reactions still need to be explored. In this work, a novel integrated downstream process involving the simultaneous PEGylation reaction and ABS extraction of four model proteins (*i.e.* cytochrome-c, lysozyme, L-asparaginase and catalase) is proposed. In these systems, the PEG–protein conjugates are used as phase-forming components in ABS, together with a citrate salt, allowing the formation of a biphasic system concurrently separating the PEGylated conjugates while simultaneously stopping the PEGylation reaction. Our results stand out as an attractive and simple *in situ* separation strategy for PEGylated proteins integrated with the bioconjugation reaction, without the need for toxic reagents such as hydroxylamine to stop the reaction.[10] This research represents a pioneering study on the integration of the PEGylation reaction and purification of protein conjugates in a single step, employing the PEGylated proteins as one of the ABS phase components, resulting in the separation of the PEGylated conjugates from the unreacted proteins by a non-chromatographic and simpler method. Following this approach, a successful integrated process was envisioned not only for a complete PEGylation reaction, but also for the most common scenario of an incomplete reaction (yield of reaction of 64%). High recovery yields and purities were achieved for the PEGylated conjugates (92% < $\%RecT_{\text{Cyt-c-PEG}}$ < 98%; 85% < purity < 100%) and for the unreacted enzyme ($\%RecB_{\text{Cyt-c}}$ = 81%; purity = 98%), thus increasing the overall sustainability of the process and meeting the principles of green chemistry.

Experimental

Materials

The four model proteins used were the horse heart cytochrome c (Cyt-c, ≈12 kDa, pI = 10.0–10.5) with a purity of ≥95% from Sigma-Aldrich (St Louis, MO), lysozyme from chicken egg white (LYS, ≈14 kDa, pI = 11.35) with a purity of ≥90% from Sigma-Aldrich, L-asparaginase from *Escherichia coli* (ASNase, ≈130 kDa, pI = 4.9) 2500 IU with a purity of ≥95% from Prospec-Tany (Ness Ziona, Israel), and catalase from bovine liver (CAT, ≈240 kDa, pI = 5.4) with a purity of ≥95% from Sigma-Aldrich.

The PEG derivatives used in the PEGylation reaction were methoxy polyethylene glycol succinimidyl NHS esters of 5, 10, 20 and 40 kDa (mPEG-NHS, purity >95%), obtained from Nanocs (New York, NY). The aqueous buffer used in the PEGylation reaction was potassium phosphate buffer (100 mM), with pH adjusted to 7 through drop-wise addition of 2 M NaOH. Potassium citrate buffer was used to stop the PEGylation reaction and to promote phase separation. The salts potassium phosphate dibasic (K_2HPO_4, 95% of purity), potassium phosphate monobasic (KH_2PO_4, 95% of purity), citric acid, ($C_6H_8O_7$, purity ≥99%) and potassium citrate tribasic monohydrate ($C_6H_5K_3O_7{\cdot}H_2O$, purity ≥99%) were purchased from Sigma-Aldrich. Polyethylene glycols (PEG) and methoxy polyethylene glycols (mPEG) for phase diagram determination were from Sigma-Aldrich with purity ≥95%.

For the chromatography mobile phase, sodium chloride, NaCl (purity ≥99%; Sigma-Aldrich), sodium phosphate dibasic, Na_2HPO_4 (purity ≥99%; Sigma-Aldrich), sodium phosphate monobasic, NaH_2PO_4, (purity ≥99%; Sigma-Aldrich), and ultrapure water treated in a Milli-Q 185 water apparatus (Millipore, Bedford, MA) were used. Syringe filters (0.45 μm pore size; Specanalitica, Portugal) and membrane filters (0.22 μm; Sartorius Stedim Biotech, Germany) were used in the filtration steps.

Phase diagrams of polyethylene glycol + citrate buffer ABS

The phase diagrams were mapped out gravimetrically, within an uncertainty of $\pm 10^{-4}$ g, using the cloud point titration method[25,26] at 298 ± 1 K and atmospheric pressure. The following systems were investigated: PEG 2, 6, 10, and 20 kDa + potassium citrate buffer (pH = 7.0) and mPEG 2 kDa + potassium citrate buffer (pH = 7.0). Briefly, two stock solutions were prepared: 50 wt% of PEG and 50 wt% of potassium citrate buffer, $C_6H_5K_3O_7/C_6H_8O_7$, pH = 7.0. Dropwise addition of buffer into the polymer solution was carried out until the visual detection of a turbid system (biphasic region). Subsequently, dropwise addition of Milli-Q water was conducted until the system became clear (monophasic region). This procedure was

repeated several times, under constant stirring and controlled temperature, to obtain the binodal curve. The experimental data were correlated using the Merchuk equation[27] to generate the phase diagrams (eqn (1)):

$$[\mathrm{PEG}] = A\exp[(B \times [\mathrm{citrate}]^{0.5}) - (C \times [\mathrm{citrate}]^{3})] \quad (1)$$

where [PEG] and [citrate] represent the weight percentages of PEG polymers and potassium citrate buffer, respectively. A, B and C are constants obtained by the regression of the experimental data. The Merchuk equation was chosen since it has a small number of adjustable parameters to correlate these data and it is most commonly applied.[27]

Combined PEGylation reaction and recovery step

The PEGylation reactions were conducted according to the literature.[28] Briefly, 300 μL of a protein solution (2 mg mL^{-1} for condition 1 and 4 mg mL^{-1} for condition 2) in potassium phosphate buffer (100 mM, pH = 7.0) was added to a flask containing 50 mg of mPEG-NHS. The mixtures were magnetically stirred at 400 rpm for 7.5 min, at room temperature (*ca.* 25 °C), and then the reaction was stopped through the drop-wise addition of 100 μL of potassium citrate buffer (pH = 7.0, 50 wt% $C_6H_5K_3O_7/C_6H_8O_7$), consequently promoting the formation of two-phase systems composed of a Prot-PEG-rich (top) phase and a salt-rich (bottom) phase. The ABS applied were composed of 0.5 wt% of Prot + 12.5 wt% of Prot-PEG/PEG + 12.5 wt% of $C_6H_5K_3O_7/C_6H_8O_7$ (condition 1) and 1.0 wt% of Prot + 12.5 wt% of Prot-PEG/PEG + 12.5 wt% of $C_6H_5K_3O_7/C_6H_8O_7$ (condition 2). The two aqueous phases were carefully separated, and their volumes were measured.

Three variables were studied to develop and optimize the integrated conjugation–recovery process, namely the (i) mPEG-NHS molecular weight, (ii) reaction time and (iii) protein type. For the first study, four mPEG-NHS polymers of 5, 10, 20 and 40 kDa were conjugated with Cyt-c at 2 mg mL^{-1} (condition 1) and 4 mg mL^{-1} (condition 2). Then, three reaction times were studied for Cyt-c PEGylation with mPEG-NHS of 20 kDa under condition 2, namely: 7.5, 15, and 30 min. Finally, to prove that this one-step approach is suitable for more than one protein, different classes of proteins were tested: small proteins (Cyt-c and LYS, <50 kDa) and large proteins (ASNase and CAT, >100 kDa). In this step, the PEGylation reaction was performed with mPEG-NHS of 20 kDa, for 7.5 min under condition 2 and the ABS formed by potassium citrate buffer addition.

Quantification of PEGylated conjugates and unreacted proteins: fractionation parameters

The concentrations of unreacted proteins (Cyt-c, LYS, ASNase, and CAT) and each conjugate (Cyt-c-PEG, LYS-PEG, ASNase-PEG, and CAT-PEG) at both top and bottom phases were determined spectrophotometrically at 280 nm after size-exclusion chromatography,[16] with a respective calibration curve for each protein and PEGylated conjugate. Samples of top and bottom phases were injected into an AKTA™ purifier system (GE Healthcare, United States) Fast Protein Liquid Chromatographer equipped with a Superdex 200 Increase 10/300 GL chromatographic column prepacked with crosslinked agarose-dextran high-resolution resin (GE Healthcare). The column was equilibrated with 0.01 M sodium phosphate buffer solution (0.14 M NaCl, pH = 7.4) and eluted with the same buffer with a flow of 0.75 mL min^{-1}. All experiments were performed in triplicate and the final concentration was reported as the average of three independent assays with the respective standard deviations calculated.

The performance of the different ABS investigated was based on the following parameters: partition coefficients in a log scale ($\log K$) and recoveries in the top (*Rec Top* – %) and bottom (*Rec Bot* – %) phases of unreacted proteins and PEGylated conjugates, eqn (2)–(4), respectively:

$$\log K = \log\left(\frac{[\mathrm{Prot}]\mathrm{top}}{[\mathrm{Prot}]\mathrm{bot}}\right) \quad (2)$$

$$Rec\ Top\,(\%) = \frac{100}{1 + \left(\frac{1}{K \times \mathrm{Rv}}\right)} \quad (3)$$

$$Rec\ Bot\,(\%) = \frac{100}{1 + \mathrm{Rv} \times K} \quad (4)$$

where [Prot]top and [Prot]bot represent the protein concentration in the top and bottom phases, respectively. Rv represents the volume ratio between the top and bottom phases.

The selectivity (S) of the systems was also determined based on eqn (5):

$$S = \frac{K_{\text{Prot-PEG}}}{K_{\text{Prot}}} \quad (5)$$

Determination of total protein concentration

The protein concentration was determined with the Pierce BCA Protein Assay and Micro BCA Protein Assay (Thermo Scientific, Schwerte, Germany) according to the product recommendations. Bovine serum albumin (albumin standard ampules, Thermo Scientific, Schwerte, Germany) was used as a standard protein.

Protein activity assays

The specific activity of the proteins in the top and bottom phases was determined and activity balances were calculated to confirm that the use of ABS was a gentle purification approach and to guarantee the maintenance of the biological activity of proteins. The specific activity, SA (U mg^{-1}), represents the ratio between the volumetric activity of the respective protein (U mL^{-1}) and the total protein concentration (mg mL^{-1}) at a certain aqueous phase (top or bottom). Every sample was measured in triplicate and the average was used to calculate the reaction rate.

Cyt-c activity

The enzymatic activity of Cyt-c was determined by the catalytic oxidation of 50 μM 2,2′-azino-bis(3-ethylbenzothiazoline-6-sulphonic acid), ABTS (Sigma–Aldrich, >98%), in the presence of

0.5 mM hydrogen peroxide (Sigma–Aldrich, solution 30 wt% in H_2O).[29,30] The samples of both top and bottom phases were diluted to obtain a protein concentration of 10 μM in 0.01 M potassium phosphate buffer (0.14 M NaCl, pH 7.4). The reaction was started by adding hydrogen peroxide and then there was an absorbance increase at 418 nm.

LYS activity

The LYS activity was determined using *Micrococcus lysodeikticus* (Sigma–Aldrich) as the substrate.[31] The kinetic assay is based on the lysis of the bacterial cells by lysozymes resulting in a decrease of turbidity over time. The *M. lysodeikticus* cells (0.015% w/v) were suspended in 50 mM sodium phosphate buffer at pH 6.24. For the diluted samples of top and bottom phases, a volume of 0.1 mL was mixed with 2.5 mL of substrate solution. Absorption measurements at 450 nm were performed for 10 min in 30 s intervals with orbital shaking in between the measurements. The diluted samples of proteins from both phases contained 200–400 U mL^{-1} of LYS. A blank consisting of 0.1 mL of sodium phosphate buffer (50 mM, pH 6.24) mixed with 2.5 mL of substrate solution was measured likewise. The absorbance values of the protein samples were subtracted from the absorbance values of the *M. lysodeikticus* blank, resulting in a positive slope of the measured values over time. One unit is equal to a decrease in turbidity of 0.001 per minute at 450 nm, pH 6.24 and 25 °C under the specified conditions.

ASNase activity

The ASNase activity was based on the protocol of Drainas and co-workers.[32] Briefly, 0.1 mL of a diluted sample (top and bottom phases), 0.7 mL of Tris-HCl buffer (50 mM, pH 8.6), 0.1 mL of ASNase (0.1 M) and 0.1 mL of hydroxylamine (1.0 M, pH 7.0) were incubated at 37 °C for 30 min. The reaction was interrupted by adding 0.5 mL of 0.31 M iron chloride reagent (dissolved in 0.33 M HCl and 0.3 M trichloroacetic acid solution, Sigma–Aldrich, >97%). The reaction solution was centrifuged at 3220*g* for 15 min and the iron chloride–hydroxamic acid complex produced was quantified at 500 nm. The calibration curve was prepared from a β-aspartohydroxamic solution (Sigma-Aldrich, MO, USA, ≥98%). One unit of ASNase activity is defined as the amount of enzyme that produces 1 μmol of β-aspartohydroxamic acid per minute under the experimental conditions defined.

CAT activity

The CAT activity was quantified by the Iwase *et al.* method that measures the trapped oxygen gas generated by the catalase–hydrogen peroxide reaction, which is visualized as foam.[33] Each CAT sample from top and bottom phases (100 μL) was added in a Pyrex tube (13 mm diameter × 100 mm height, borosilicate glass; Corning, USA). Subsequently, 100 μL of 1% Triton X-100 (Sigma–Aldrich, 98%) and 100 μL of undiluted hydrogen peroxide (Sigma–Aldrich, solution 30 wt% in H_2O) were added to the CAT samples, mixed thoroughly and then incubated at room temperature. The CAT samples from top and bottom phases were diluted to stay in the linearity range of 20–300 units (U) of catalase activity. Following completion of the reaction, the height of O_2-forming foam that remained constant for 15 min in the test tube was finally measured using a ruler and correlated with the CAT concentration based on a calibration curve.

FTIR-ATR spectrum acquisition

The Fourier Transform Infrared Spectroscopy (FTIR) profiles of standards (Cyt-c, model protein and PEG) and top and bottom phases were recorded using an FT RAMAN BRUKER 100/S spectrometer (Bruker, Billerica, MA) in mid-IR mode, equipped with a Universal ATR (attenuated total reflectance) sampling device containing a diamond/ZnSe crystal. For powdered samples, an extra accessory plate with a conic awl was used, requiring only a few milligrams, without any previous sample preparation. The pressure applied to squeeze the powdered sample towards the diamond was approximately 148 ± 1 N. The spectra were scanned at room temperature in absorbance mode over the wave number range of 4000 to 50 cm^{-1}, with a scan speed of 0.20 cm s^{-1}, and 30 accumulations at a resolution of 4 cm^{-1}. Triplicates of each sample were averaged to obtain an average spectrum. A background spectrum of air was scanned under the same instrumental conditions before each series of measurements. The spectra acquired were processed with the Spectrum software version 6.3.2.

Electrophoresis in polyacrylamide gel

Top and bottom phase samples were analysed by SDS-PAGE to detect the presence of PEGylated and unreacted proteins in both aqueous phases. Proteins were stained with Coomassie Brilliant Blue. Electrophoretic gel for separation was prepared with 522 mM Tris-HCl (pH 8.8), 6%, 10% or 12% of acrylamide/bis-acrylamide, 0.09% (w/v) of ammonium persulphate (PSA), and 0.19% (v/v) of tetramethylethylenediamine (TEMED). The packing gel was prepared with 116 mM Tris-HCl (pH 6.8), 5% of acrylamide/bis-acrylamide, 0.14% (w/v) of PSA, and 0.29% (v/v) of TEMED. For SDS-PAGE, 0.1% (w/v) of sodium dodecyl sulphate (SDS) was added to the gels. Samples were prepared with 4× of protein buffer and 25 mM dithiothreitol (DTT) for SDS-PAGE. The running buffer was Tris-Glycine/SDS 1× (pH 8.3) for SDS-PAGE and the gel was kept under 80 mA at room temperature (22 to 25 °C). The SDS-PAGE gels are depicted in Fig. S2 in the ESI.†

Results and discussion

Phase diagrams and selection of the mixture point for ABS preparation

Novel ternary phase diagrams were determined for the systems used in the integrated step (polyethylene glycol + $C_6H_5K_3O_7$/$C_6H_8O_7$ pH = 7 + water, 298 ± 1 K) to define a biphasic region and, consequently, to choose a mixture point corresponding to phase separation of a top phase rich in PEG and a bottom one rich in salt. Citrate-based salts were chosen since they are bio-

degradable and nontoxic, with a strong salting-out ability.[34] The detailed experimental weight fraction data, Merchuk correlation parameters (*A*, *B* and *C*) and graphical representations of phase diagrams in mass fraction are reported in the ESI (Tables S1, 2 and Fig. S1†). In the downstream process proposed to integrate the PEGylation reaction with the fractionation by ABS, the PEGylated protein is expected to work as one of the phase forming components. Since the grafted PEG groups are methoxylated and no previous reports on mPEG phase diagrams are available, novel experimental phase diagrams were mapped out. The phase diagrams for polyethylene glycol (PEG) and mPEG with the same molecular weight (2 kDa) + $C_6H_5K_3O_7$/$C_6H_8O_7$ (pH = 7) were studied and similar binodal curves were obtained (Fig. S1A†). Therefore, the methoxy group of the polymer chain has a negligible effect regarding the two-phase formation capability, and for larger polymer sizes an equivalent trend is observed. Based on this result, phase diagrams of PEG/citrate systems were mapped out for regular PEGs of 2, 6, 10, and 20 kDa (Fig. S1B†). As extensively described in the literature, for PEG/salt-based ABS, the increase of molecular weight contributes to a higher capacity to induce phase separation due to the hydrophobicity of the phase formed by longer polymeric PEG chains.[35,36] Based on the phase diagrams, a biphasic mixture point was chosen for the PEGylation reaction media (12.5 wt% of PEG + 12.5 wt% $C_6H_5K_3O_7$/$C_6H_8O_7$ pH = 7). This mixture point corresponds to the biphasic region in all phase diagrams evaluated (PEGs: 6–20 kDa).

Process optimization

PEG/salt-based ABS are highlighted as promising for the recovery of PEGylated proteins, *i.e.* bovine serum albumin,[37,38] Cyt-c,[16] RNase A,[17,18,39] lactoalbumin,[17] LYS,[40] immunoglobulin G,[37] and granulocyte-macrophage colony stimulation factor.[37,38] Nevertheless, the direct application of this operation in reaction media has not been extensively studied. The only previous report refers to an *in situ* ABS strategy formed by adding 4 mol L^{-1} ammonium sulphate in 20 mmol L^{-1} Tris-HCl (pH 7.0) to lysozyme PEGylation reactions.[15] In this study, several polymers and salt solutions were tested as potential phase-forming agents with the further analysis of the LYS-PEG and LYS partitioning behaviour. This manuscript provides some insights into the possibility of conceiving a unidirectional and integrative process in the production of PEGylated proteins at large reaction volumes, which cannot be processed using packed bed or on-column PEGylation processes due to the limiting saturation capacities of the large columns. Yet, the need to deeply explore the *in situ* potential of ABS in PEGylation reactions still demands to be addressed. Moreover, the idea of an integrative approach combining the bioconjugation reaction and ABS recovery, without the use of toxic reagents such as hydroxylamine to stop the reaction, and without the addition of more quantities of PEG to promote the phase separation is still a challenge. Given the well-established versatility of ABS regarding their integration capacity for chemical reactions in one-step and one-pot processes,[41,42] we investigated the full one-step potential of ABS combining PEGylation reaction and protein conjugate purification. The effect of the size of the reactive PEG on the integrated purification stage, the influence of the reaction time in the *in situ* ABS for recovery of PEGylated proteins, and the proof of concept by investigating several proteins (with small and large sizes) were investigated.

Initially, mPEG-NHS of different molecular weights (5, 10, 20, and 40 kDa) were used for the PEGylation of Cyt-c. After PEGylation, the addition of a salt promoted the phase separation with the top phase rich in PEGylated proteins (phase-forming compound) and an excess of mPEG, while the bottom phase is rich in the potassium citrate salt, in which the unreacted proteins preferentially partitioned. Table 1 presents the values of the volume ratio (V_R) and recovery parameters for Cyt-c and Cyt-c-PEG, *i.e.* *K*, %*RecT*, %*RecB*, and *S* for both experimental conditions. Fig. 1 shows the data of *S* and the logarithm function of *K* obtained after the study of two distinct protein concentrations (0.5 wt% and 1.0 wt% of protein, conditions 1 and 2, respectively) and different conditions of the PEG MW, reaction time and type of protein. The positive values of log *K* depicted in Fig. 1 indicate the partition preference of the protein towards the top phase, while negative values indicate its preference for the bottom phase. *S* values above 1000 were represented as >1000, indicating the complete separation of PEGylated proteins from the unreacted protein.

Table 1 Effect of the molecular weight (MW) of mPEG-NHS upon the volume ratio (V_R) and partitioning behaviour, represented as the partition coefficient (*K*), top and bottom-phase recoveries (%*RecT* and %*RecB*), and selectivity (*S*) of native and PEGylated Cyt-c in Cyt-c-PEG + potassium citrate buffer-based ABS

MW mPEG-NHS	V_R	$K_{Cyt\text{-}c}$	$K_{Cyt\text{-}c\text{-}PEG}$	*S*	$\%RecT_{Cyt\text{-}c}$ (%)	$\%RecB_{Cyt\text{-}c}$ (%)	$\%RecT_{Cyt\text{-}c\text{-}PEG}$ (%)	$\%RecB_{Cyt\text{-}c\text{-}PEG}$ (%)
Condition 1: *0.5 wt% Cyt-c + 12.5 wt% Cyt-c-PEG + 12.5 wt% potassium citrate buffer*								
mPEG 5 kDa	0.46	0.00072 ± 0.00004	4.5 ± 0.2	>1000	0	100	90.7 ± 0.5	9.3 ± 0.5
mPEG 10 kDa	0.52	0.0051 ± 0.0003	2.2 ± 0.1	426	0.3 ± 0.1	99.7 ± 0.1	81 ± 1	19 ± 1
mPEG 20 kDa	0.73	0.115 ± 0.06	7 ± 0.4	61	7.8 ± 0.7	92.3 ± 0.7	90.6 ± 0.5	9.4 ± 0.5
mPEG 40 kDa	0.81	0.204 ± 0.01	31 ± 2	154	14.2 ± 0.7	85.8 ± 0.7	97.5 ± 0.1	2.5 ± 0.1
Condition 2: *1.0 wt% Cyt-c + 12.5 wt% Cyt-c-PEG + 12.5 wt% potassium citrate buffer*								
mPEG 5 kDa	0.52	0.038 ± 0.002	3.3 ± 0.2	87	1.9 ± 0.1	98.1 ± 0.1	86.4 ± 0.7	13.6 ± 0.7
mPEG 10 kDa	0.58	0.090 ± 0.005	10.8 ± 0.5	119	5.0 ± 0.3	95.0 ± 0.3	94.9 ± 0.3	5.1 ± 0.3
mPEG 20 kDa	0.90	0.108 ± 0.005	13.3 ± 0.7	123	8.9 ± 0.4	91.1 ± 0.4	93.6 ± 0.3	6.4 ± 0.3
mPEG 40 kDa	2.17	0.109 ± 0.005	25 ± 1	233	19 ± 1	81 ± 1	92.1 ± 0.4	7.9 ± 0.4

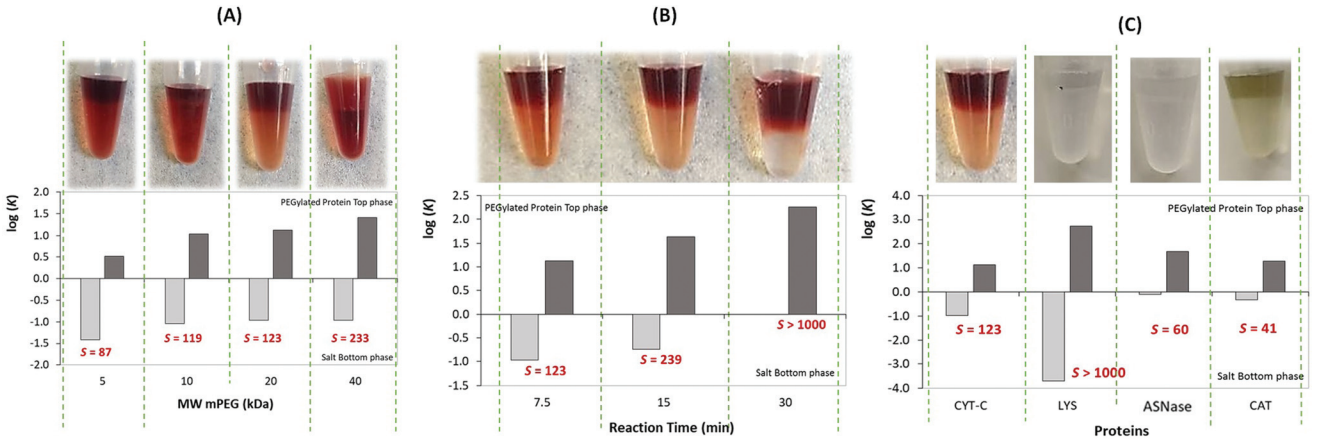

Fig. 1 Logarithmic function of K for both native (light grey bars) and PEGylated proteins (dark grey bars) in the *in situ* approach under development for the system composed of 1.0 wt% protein (condition 2) + 12.5 wt% Prot-PEG/PEG + 12.5 wt% potassium citrate buffer, at pH = 7. The selectivity of each system (S) is presented in red. Pictures of each ABS prepared are depicted for each system.

Our results show that V_R tends to increase with the PEG MW (*i.e.* $0.46 \leq V_R \leq 0.81$, condition 1) resulting in the increase of the upper volume of the top phase rich in PEGylated protein. In the range of PEG MWs studied (Table 1 and Fig. 1A), higher selectivity values were obtained ($S \geq 61$ and $S \geq 87$, for conditions 1 and 2, respectively). In this sense, the unreacted protein partitioned preferentially into the bottom phase, predominantly in the systems with PEGs of smaller MWs (%$RecB_{\text{Cyt-c}}$ > 85% for mPEG 40 kDa, %$RecB_{\text{Cyt-c}}$ = 100% for mPEG 5 kDa, condition 1). Moreover, the PEGylated protein migrates to the top phase, preferentially for systems with larger PEG MWs (%$RecT_{\text{Cyt-c-PEG}}$ > 90% for mPEG 5 kDa, %$RecT_{\text{Cyt-c-PEG}}$ > 97% for mPEG 40 kDa, condition 1). Indeed, PEGylated Cyt-c is one of the main phase forming agents. Partition results were similar for both initial Cyt-c concentrations studied (conditions 1 and 2, respectively). Nonetheless, PEGylation yields were higher for condition 1 as a consequence of the higher mPEG-NHS : protein molar ratio.

The effect of PEGylation reaction time was investigated for 1.0 wt% of Cyt-c (condition 2). As can be seen in Fig. 1B and Table 2, high selectivity values were observed for all reaction times. The increase of the reaction time resulted in higher PEGylation yields, with 100% of Cyt-c-PEG for the longer time of reaction (t = 30 min). Herein, for the complete reaction, the ability of this system to concentrate the PEGylated conjugates in the aqueous phase is also demonstrated. As a result, the top-phase volume increases with the reaction time ($0.90 \leq V_R \leq 2.80$), as can be seen from the photographs in Fig. 1. Likewise, the recovery yields are enhanced with the extension of the reaction (%$RecT_{\text{Cyt-c-PEG}}$ = 98.5 ± 0.1% for 30 min, %$RecT_{\text{Cyt-c-PEG}}$ = 93.6 ± 0.3% for 7.5 min). Additionally, the efficiency of adding potassium citrate to end the PEGylation reaction was proved, since different degrees of PEGylation were achieved after adding it at distinct reaction times. Therefore, it represents a non-toxic and eco-friendly alternative to replace hydroxylamine as a reagent to stop PEGylation.

Aiming at proving the transversal potential of integrating the PEGylation reaction and primary recovery as an alternative approach, three other enzymes were tested. The chromatograms of both top and bottom phases of all systems are depicted in Fig. S3–S5 in the ESI† for each studied protein, reflecting the products partitioning in both phases. The fractionation parameters for the native and PEGylated proteins were calculated by peak integration (*i.e.* K, %Rec, and S). In this sense, the mixture point (1.0 wt% of protein + 12.5 wt% Prot-PEG + 12.5 wt% potassium citrate buffer, pH = 7.0) previously selected was tested for LYS, ASNase and CAT, using the PEG of 20 kDa (Table 3 and Fig. 1C). Again, the preferential behaviour of native proteins towards the salt-rich phase and the PEGylated species towards the top phase was observed with no exceptions. Nonetheless, a more selective performance was found for Cyt-c and LYS (smaller proteins), with S values

Table 2 Effect of PEGylation reaction time on the volume ratio (V_R) and partition behaviour, represented as the partition coefficient (K), top and bottom-phase recoveries (%$RecT$ and %$RecB$), and selectivity (S) of native and PEGylated Cyt-c in ABS composed of 1.0 wt% Cyt-c + 12.5 wt% Cyt-c-PEG/PEG + 12.5 wt% potassium citrate buffer, at pH 7.0

Time (min)	V_R	$K_{\text{Cyt-c}}$	$K_{\text{Cyt-c-PEG}}$	S	%$RecT_{\text{Cyt-c}}$ (%)	%$RecB_{\text{Cyt-c}}$ (%)	%$RecT_{\text{Cyt-c-PEG}}$ (%)	%$RecB_{\text{Cyt-c-PEG}}$ (%)
7.5	0.90	0.108 ± 0.005	13.3 ± 0.7	123	8.9 ± 0.4	91.1 ± 0.4	93.6 ± 0.3	6.4 ± 0.3
15	1.24	0.181 ± 0.009	43 ± 2	239	18.3 ± 0.9	81.7 ± 0.9	97.2 ± 0.1	2.8 ± 0.1
30	2.80	[a]	181 ± 9	>1000	[a]	[a]	98.5 ± 0.1	1.5 ± 0.1

[a] Absence of unreacted Cyt-c since at 30 min the complete PEGylation reaction occurs.

Table 3 Partition parameters for Cyt-c, LYS, ASNase, and CAT for the *in situ* approach bioconjugation + ABS approach: volume ratio (V_R), partition coefficient (K), top and bottom-phase recoveries (*%RecT* and *%RecB*), and selectivity (S) of native and PEGylated enzyme conjugates in ABS composed of 1.0 wt% protein + 12.5 wt% Prot-PEG/PEG + 12.5 wt% potassium citrate buffer, performed with mPEG-NHS of 20 kDa for a reaction time of 7.5 min

Proteins	V_R	K_{PROT}	$K_{PROT\text{-}PEG}$	S	$\%RecT_{PROT}$ (%)	$\%RecB_{PROT}$ (%)	$\%RecT_{PROT\text{-}PEG}$ (%)	$\%RecB_{PROT\text{-}PEG}$ (%)
Cyt-c	0.90	0.108 ± 0.005	13.3 ± 0.7	123	8.9 ± 0.4	91.1 ± 0.4	93.6 ± 0.3	6.4 ± 0.3
LYS	0.73	0.0002 ± 0.0001	543 ± 27	>1000	0	100	100	0
ASNase	0.90	0.79 ± 0.04	47 ± 2	60	42 ± 2	58 ± 2	98.1 ± 0.1	1.9 ± 0.1
CAT	1.11	0.46 ± 0.02	19 ± 1	41	34 ± 2	66 ± 2	94.4 ± 0.3	5.6 ± 0.3

of 123 and >1000, respectively. In the case of LYS, a complete separation was achieved ($\%RecB_{LYS}$ = 100% and $\%RecT_{LYS\text{-}PEG}$ = 100%) by our one-step *in situ* approach. Regarding the larger enzymes, higher recovery yields were obtained for PEGylated conjugates towards the top phase, but recovery yields of the unreacted protein towards the opposite phase were lower (94% > $\%RecT_{PROT\text{-}PEG}$ > 98%, 58% > $\%RecB_{PROT}$ > 66%). This decrease of the recovery yield of the unreacted protein in the salt-rich phase may be a result of its higher molecular weight and consequent protein partition to the top phase by a salting-out phenomenon caused by the presence of the potassium citrate salt.[43]

The partition of the PEGylated protein to the top phase was also tested by electrophoresis, performed in the protein type and time assays (Fig. S2 in the ESI†). Accordingly, the top phases are constituted mainly by PEGylated proteins (bands with higher molecular weight), while the bottom phases correspond only to the native protein (Fig. S2A†). Moreover, for longer times (t > 15 min) the relative band of the unmodified protein (Cyt-c) is not present, meaning that the reaction becomes complete (*i.e.* PEGylation yield = 100%) (Fig. S2B†).

While developing a strategy to efficiently produce PEGylated enzymes and purify them from the respective unreacted protein, the ABS used in this work proved to be simultaneously able to maintain the activity and structural integrity of each model enzyme. The enzyme activity was evaluated in both top and bottom phases, to guarantee the biological activity of both PEGylated and unreacted enzymes, since we expected to increase the sustainability of the process by reintroducing the unreacted enzyme in new cycles of the PEGylation reaction.[16] Table 4 presents the specific activity (SA, U mg^{-1}) and the volumetric activity (A, U mL^{-1}) for each enzyme species concentrated in both top and bottom phases. In all cases, the enzyme activity was preserved, emphasizing the biocompatible and mild nature of the downstream process envisioned in this work.

Moreover, and due to the sensitivity of the enzymes to small changes in their secondary structure, Fourier transform infrared spectroscopy (FTIR) was also performed to investigate PEG–protein bioconjugation and partition. Fig. 2 shows the FTIR spectra of pure PEG and Cyt-c together with ABS top and bottom phases after PEGylation and phase separation. As observed, the IR spectra present three main spectral regions resulting from a complex combination of vibration modes from different infrared-activated functional groups typical of PEG and Cyt-c IR fingerprints: 3500–2700 cm^{-1}, 1700–1500 cm^{-1} and 1500–1000 cm^{-1}.[44,45] The appearance of two bands at 2921 and 2883 cm^{-1} assigned to aliphatic C–H asymmetric and symmetric stretching of PEG methylene groups at the top Cyt-c confirms the success of the PEGylation reaction while also demonstrating the presence of Cyt-c-PEG as the main component of the top-phase of ABS.[46] This is further supported by the occurrence of a broad envelope with the maximum intensity centered at 1085 cm^{-1}, resulting from a band merging effect assigned to the combination of C–O and C–O–C stretching and C–O–H bending vibrations of the attached PEG.[44] The amide I band present at 1638 cm^{-1} representing the C–O stretching vibrations of the peptide group, the amide II band at 1578 cm^{-1} corresponding primarily to N–H bending and contributions of C–N stretching vibrations, and the amide III band at 1388 cm^{-1} representing the N–H bending and C–N stretching vibrations prove that Cyt-c retains its secondary structure after PEGylation.[47] Despite the fact that no changes are observed in the vibrational frequency of the studied proteins, an increase of the intensity of amide I when compared with that of amide II is observed for the ABS top phase, and when compared with the data for both the pure Cyt-c and bottom phase of the ABS.

Table 4 Total protein concentration ([P]), specific activity (SA) and volumetric activity of the protein in the top and bottom phases (T and B subscripts, respectively) for Cyt-c, LYS, ASNase, and CAT in the *in situ* process under development for the ABS composed of 1.0 wt% protein + 12.5 wt% Prot-PEG/PEG + 12.5 wt% potassium citrate buffer, performed with mPEG-NHS of 20 kDa for a reaction time of 7.5 min

Proteins	$[P]_T$ (mg mL^{-1})	$[P]_B$ (mg mL^{-1})	A_T (U mL^{-1})	A_B (U mL^{-1})	SA_T (U mg^{-1})	SA_B (U mg^{-1})
Cyt-c	0.352	0.070	1.11	0.17	3.15	2.40
LYS	0.437	0.039	2.55×10^3	5.52×10^3	5.84×10^3	1.43×10^5
ASNase	0.174	0.044	1.56×10^1	2.78×10^1	8.97×10^1	6.28×10^2
CAT	0.182	0.064	6.84×10^4	1.22×10^4	3.76×10^5	1.91×10^5

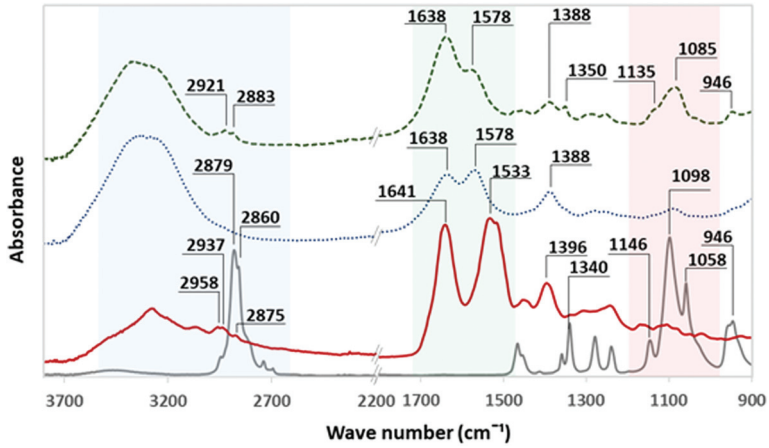

Fig. 2 FTIR-ATR spectra of pure Cyt-c (—), mPEG (—), the top-phase (---) and the bottom-phase (•••) of 1.0 wt% Cyt-c + 12.5 wt% Cyt-c-PEG/PEG + 12.5 wt% potassium citrate buffer, recorded with mPEG-NHS of 20 kDa for a reaction time of 7.5 min.

The principal objective of this work is the efficient separation of the PEGylated proteins from the native proteins in a one-pot approach combining the bioconjugation reaction with the protein conjugate purification. Currently, several bioconjugated proteins are commercialized through random PEGylation and the separation of PEGylated proteins from non-PEGylated proteins is still a challenge. The use of mPEG-NHS is characterized to commonly produce a heterogeneous mixture of PEGylated proteins with high polydispersity, since reactive PEG is bound in different lysine residues (ε-amino PEGylation). For CAT, LYS, and ASNase, only poly-PEGylated conjugates were obtained, typical of the mPEG-NHS reactions with stoichiometric excess and no pH specific control for N-terminal PEGylation. Regarding Cyt-c PEGylation, using 5 kDa mPEG-NHS, site-specific (*i.e.* Cyt-c-PEG-4 and Cyt-c-PEG-8, respectively, with 4 and 8 PEGs attached to the protein in lysine sites) and poly-dispersed conjugates were obtained as previously described by our research group.[16] Fig. 3 shows the profile of PEGylated products present in the top and bottom aqueous phases, along with the respective FPLC chromatogram. As can be seen, the site-directed PEGylated forms partition preferentially towards the bottom phase (*i.e.* 52.4% and 37.4% of Cyt-c-PEG-4 and Cyt-c-PEG-8 from all the Cyt-c-PEG conjugates), whereas the poly-PEGylated forms are mostly recovered in the opposite top phase (*i.e.* the top phase is only composed of Cyt-c-Poly-PEG). As Cyt-c bioconjugation reactions provide a higher yield of poly-PEGylated forms, the recovery of total PEGylated forms for the top phase (%$RecT_{\text{Cyt-c-PEG}}$) is higher along the side with the partition coefficient $K_{\text{Cyt-c-PEG}}$, as shown in Table 1. This differential partition of PEGylated conjugates, depending on the site-specificity correlates with the amount of PEG molecules attached to the protein. The higher the number of PEG molecules attached to the protein, the greater the partition coefficient. Thus, these results strongly suggested that there is more interaction of the PEG molecules of the poly-PEGylated conjugates among themselves, rather than with the PEG molecules of the site-directed PEGylated conjugates, which partition preferentially to the more hydrophilic phase, as previously observed in another study.[16] The purification of site-specific PEGylated conjugates (*i.e.* separation of Cyt-c-PEG-4 from Cyt-c-PEG-8) was not intended to be done through this approach, since this aim has already been addressed in one of our previous studies.[16]

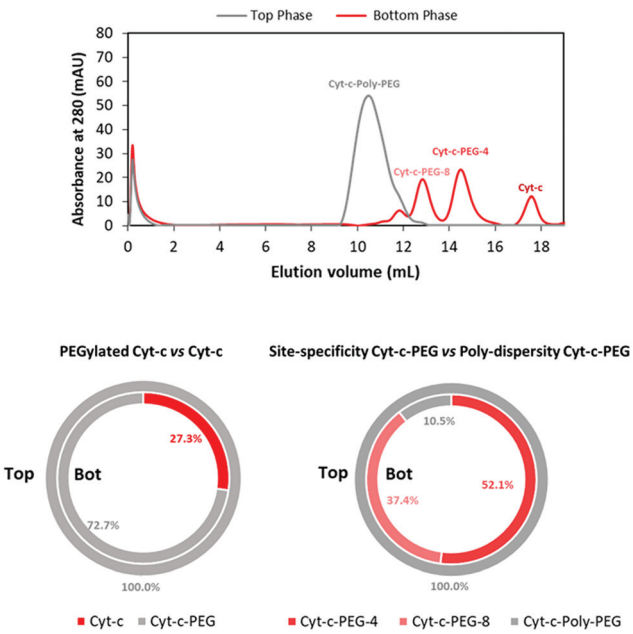

Fig. 3 PEGylated product distribution in the top and bottom phases, highlighting the site-specificity *vs.* poly-dispersity of the PEGylation reaction in the system 1.0 wt% Cyt-c + 12.5 wt% Cyt-c-PEG/PEG + 12.5 wt% potassium citrate buffer, using mPEG-NHS 5 kDa. The SEC-FPLC chromatogram of both phases is also depicted in this figure.

Diagram of the integrated process combining bioconjugation reaction and protein form separation

Three of the main criteria for the development of a sustainable process combining reaction and separation allied with the green chemistry principles are the (i) need for a high

yield of reaction, (ii) the possible recycling of the main unreacted reagents and (iii) the possible recycling of the main solvents. In this work, a schematic diagram (Fig. 4 and 5) is provided combining the PEGylation reaction with the purification of the protein conjugates. Here, two scenarios are considered. In the first one the PEGylation reaction is complete (1.0 wt% of Cyt-c + mPEG-NHS-20 kDa, 30 min), thus eliminating the need to recycle the unreacted enzyme (Fig. 4). The second scenario (the worst but most common one) describes an incomplete PEGylation reaction (1.0 wt% of Cyt-c + mPEG-NHS-40 kDa, 7.5 min) for which the recycling of the unreacted enzyme was contemplated in the approach (Fig. 5). In both cases, the dual role of the citrate salt was verified, namely as a phase-forming solvent, but firstly, as an agent acting to stop the PEGylation reaction, which also contributes towards the higher sustainability of the process. Moreover, for

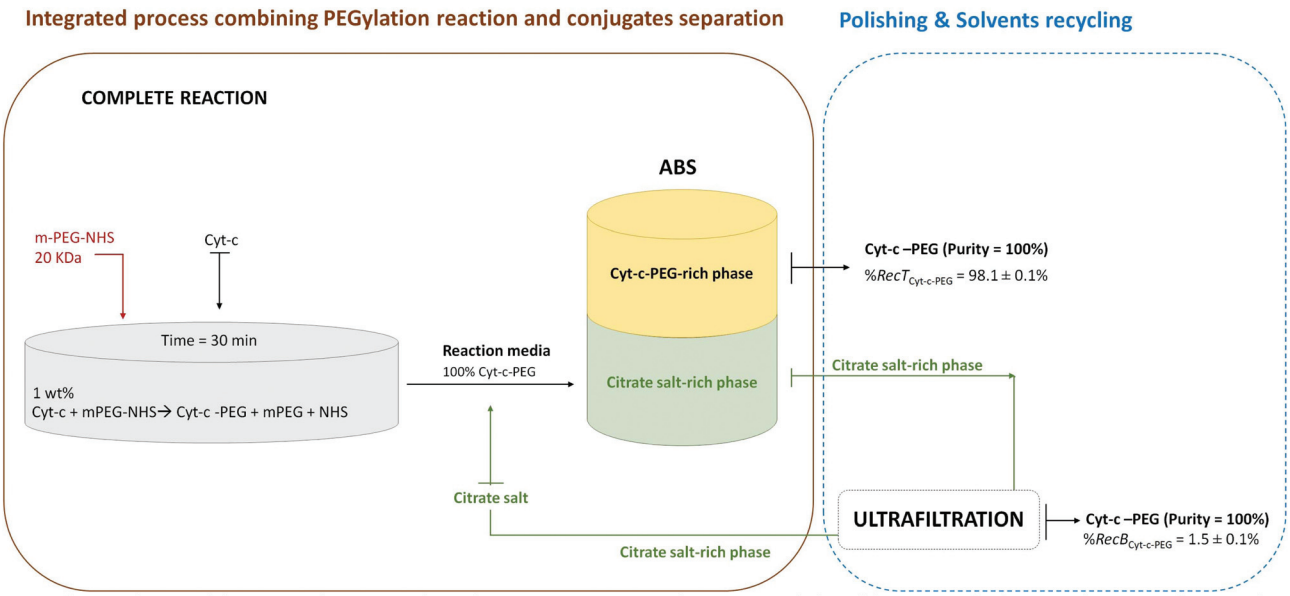

Fig. 4 Schematic diagram of the integrated process combining the bioconjugation reaction and separation with the polishing step and solvent recycling process for a complete PEGylation reaction. The dashed line represents steps that were not experimentally developed.

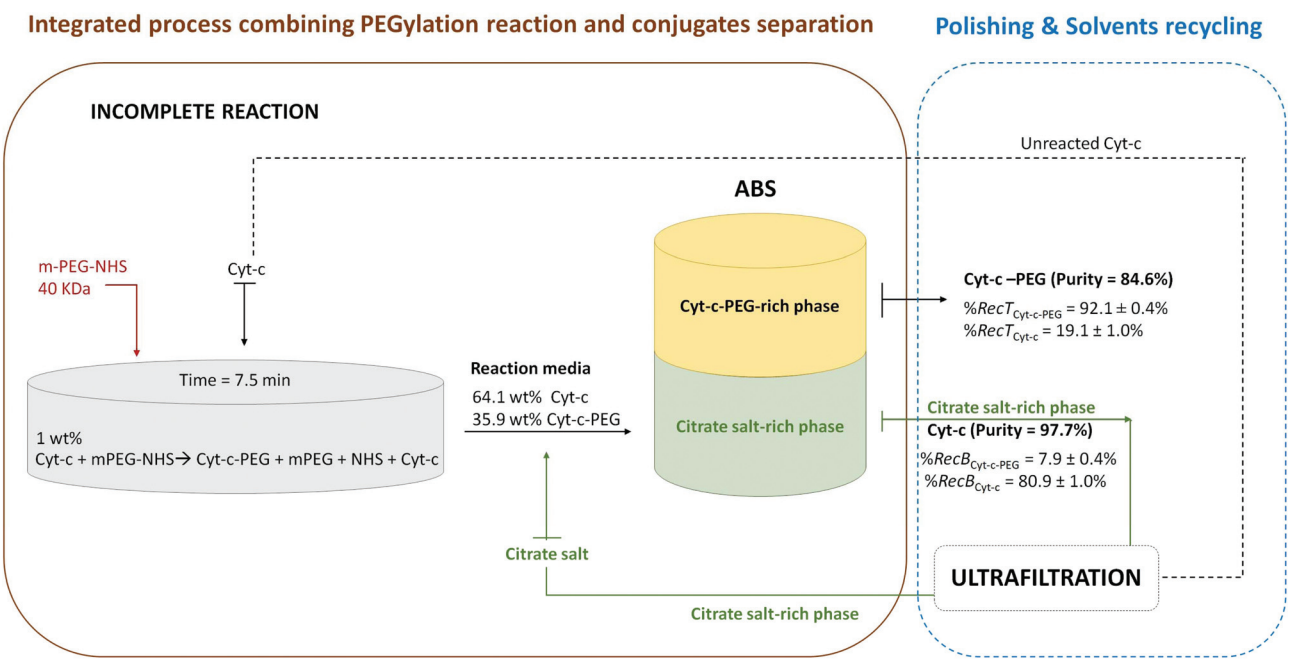

Fig. 5 Schematic diagram of the integrated process combining the bioconjugation reaction and separation with the polishing step and solvent recycling process for an incomplete PEGylation reaction. The dashed line represents steps that were not experimentally developed.

both scenarios, the yields of the reactions, as well as the recovery yields of both enzyme conjugates and unreacted enzyme (for the incomplete reaction), are represented in the respective diagram for both top and bottom phases. When the complete reaction is evaluated (Fig. 4), the process is simpler, since after the reaction (PEGylation yield of 100%) the only demand is for the separation of the enzyme bioconjugates by ABS, followed by the recycling of the phase-forming solvents, which can be easily achieved by performing ultrafiltration. Using this approach, the isolation of the citrate salt-rich phase from PEGylated Cyt-c is accomplished with success. Since the presence of the Cyt-c-PEG conjugate is only residual (around 1.5%), the salt can be directly reintroduced in the process for new cycles of PEGylation + separation. Regarding the presence of mPEG-NHS, this compound is rapidly hydrolysed in aqueous media and should be present only in residual amounts in the PEG-rich phase. If necessary, it could be removed in a polishing step by ultrafiltration or size exclusion chromatography, depending on the protein application. On the other hand, the reactive PEG hydrolysis and conjugation with the protein generate *N*-hydroxysuccinimide (NHS) and this by-product is present in both phases. While it can be removed from the PEG-rich phase in the polishing step, the NHS concentration in the salt-rich phase is much lower than the citrate concentration and does not interfere with a further ABS step after recycling. Nonetheless, one could recover the citrate after NHS accumulation by successive recycling with the addition of Ca^{2+}, resulting in calcium citrate precipitation.

Despite the good performance of this approach, the second scenario contemplating an incomplete reaction is the most common one (Fig. 5). Here, in addition to the recycling of the phase-forming solvents, the recycling and reuse of the unreacted enzyme in a new cycle of PEGylation were also contemplated. In this case, higher selectivity values were found for higher purity of both the PEGylated conjugates (purity = 84.6%) in the top phase and unreacted proteins (purity = 97.7%) in the bottom phase. Nevertheless, in both scenarios, the waste production was prevented by the addition of a recycling process using ultrafiltration, simultaneously allowing the reuse of (i) phase-forming components (citrate salt) in a consequent *in situ* ABS purification, and (ii) unreacted protein for a novel PEGylation reaction, thus contributing towards the higher sustainability and lower economic impact of the overall process. Allied with the good performance of the processes envisioned in this work, an enhanced capacity to improve the production of higher amounts of purified PEGylated proteins was achieved. The strategy developed in this work combined the higher efficiency in the recovery of PEGylated proteins with the possibility to re-use the unreacted protein and the phase forming compounds (*i.e.* potassium citrate salt) to perform a second reaction.[16] In the end, an advantageous integrated process, in comparison with chromatographic techniques, is demonstrated here, since the saturation limitations, especially in a large scale[48] described for chromatography, were eliminated.

Conclusions

In an era where the demand for more sustainable, cheap and "green" downstream processes is increasing, the need for improved downstream approaches is crucial. In this work, an alternative process was envisioned, by integrating the enzyme PEGylation with the separation of conjugates and unreacted enzyme. Aiming at simplifying the process, the PEGylated enzyme produced was used as one of the phase-forming agents, allowing the two-phase split after the direct addition of potassium citrate buffer. Despite the dual role of the enzyme conjugates as the product of the reaction and phase forming agent, the citrate salt also acts as a phase-forming agent, but firstly it is used to stop the PEGylation reaction, thus simplifying the process and avoiding the need for extra chemicals in the reaction media. After optimization of the main conditions of reaction (time of reaction and PEG MW), an integrated process was successfully achieved for four model proteins, namely Cyt-c, LYS, ASNase and CAT.

Envisioning the industrial potential of the processes developed in this work, the schematic representation of the process diagram was provided combining PEGylation reaction with purification. Two different scenarios were contemplated here, the first one representing a complete PEGylation reaction (1.0 wt% of Cyt-c + mPEG-NHS-20 kDa, 30 min), and the second and most common one representing an incomplete PEGylation reaction (1.0 wt% of Cyt-c + mPEG-NHS-40 kDa, 7.5 min). For both approaches, high recovery yields and purities were achieved for the PEGylated conjugates ($92.1 \pm 0.4\% < \%RecT_{\text{Cyt-c-PEG}} < 98.1 \pm 0.1\%$; $84.6\% <$ purity $< 100\%$) and for the unreacted enzyme ($\%RecB_{\text{Cyt-c}} = 81 \pm 1\%$; purity = 97.7%), while maintaining their structural integrity.

The findings reported here open a new pathway for the application of integrated bioconjugation + purification using ABS for the recovery of high-value biological products, such as therapeutic proteins and biosensors from larger reaction volumes, without compromising the success of the downstream process.

Conflicts of interest

There are no conflicts of interest to declare.

Acknowledgements

The authors are grateful for the financial support of the São Paulo Research Foundation-FAPESP (grants # 2018/25994-2, 2016/22065-5 and 2013/08617-7), the National Council for scientific and Technological Development-CNPq and the Coordination of Improvement of Higher Level Personnel-CAPES (Project # 001). The authors also acknowledge the FCT/MEC (Portugal) for a contract under Investigador FCT 2015 contract number IF/00402/2015 and FCT Ref. UID/CTM/50011/2019.

References

1 M. M. Zhu, M. Mollet, R. S. Hubert, Y. S. Kyung and G. G. Zhang, in *Handbook of Industrial Chemistry and Biotechnology*, 2017, pp. 1639–1669.
2 J. K. Ryu, H. S. Kim and D. H. Nam, *Biotechnol. Bioprocess Eng.*, 2012, **17**, 900–911.
3 P. H. Carter, E. R. Berndt, J. A. Dimasi and M. Trusheim, *Nat. Rev. Drug Discovery*, 2016, **15**, 673–674.
4 Y. Gong, J. C. Leroux and M. A. Gauthier, *Bioconjugate Chem.*, 2015, **26**, 1172–1181.
5 G. T. Hermanson, in *Bioconjugate Techniques (Third Ed.)*, 2013, pp. 229–258.
6 S. I. Presolski, V. P. Hong and M. G. Finn, *Chem. Biol.*, 2011, **3**, 153–162.
7 A. B. Sassi, R. Nagarkar and P. Hamblin, in *Novel Approaches and Strategies for Biologics, Vaccines and Cancer Therapies*, 2015, pp. 199–217.
8 A. Beck, S. Sanglier-Cianférani and A. Van Dorsselaer, *Anal. Chem.*, 2012, **84**, 4637–4646.
9 J. H. P. M. Santos, K. M. Torres-Obreque, G. M. Pastore, B. P. Amaro and C. O. Rangel-Yagui, *Braz. J. Pharm. Sci.*, 2018, **54**, e01009.
10 M. J. Roberts, M. D. Bentley and J. M. Harris, *Adv. Drug Delivery Rev.*, 2012, **64**, 116–127.
11 S. Jevševar, M. Kunstelj and V. G. Porekar, *Biotechnol. J.*, 2010, **5**, 113–128.
12 G. Pasut and F. M. Veronese, *J. Controlled Release*, 2012, **161**, 461–472.
13 J. González-Valdez, M. Rito-Palomares and J. Benavides, *Anal. Bioanal. Chem.*, 2012, **403**, 2225–2235.
14 J. Morgenstern, P. Baumann, C. Brunner and J. Hubbuch, *Int. J. Pharm.*, 2017, **519**, 408–417.
15 L. A. Mejía-Manzano, K. Mayolo-Deloisa, C. Sánchez-Trasviña, J. González-Valdez, M. González-González and M. Rito-Palomares, *J. Chem. Technol. Biotechnol.*, 2017, **92**, 2519–2526.
16 J. H. P. M. Santos, G. Carretero, J. A. P. Coutinho, C. O. Rangel-Yagui and S. P. M. Ventura, *Green Chem.*, 2017, **19**, 5800–5808.
17 J. González-Valdez, L. F. Cueto, J. Benavides and M. Rito-Palomares, *J. Chem. Technol. Biotechnol.*, 2011, **86**, 26–33.
18 J. González-Valdez, M. Rito-Palomares and J. Benavides, *Biotechnol. Prog.*, 2013, **29**, 378–385.
19 R. Hatti-Kaul, *Mol. Biotechnol.*, 2001, **19**, 269–277.
20 J. H. P. M. Santos, J. P. Trigo, É. Maricato, C. Nunes, M. A. Coimbra and S. P. M. Ventura, *ACS Sustainable Chem. Eng.*, 2018, **6**, 14042–14053.
21 H.-O. Johansson, M. Ishii, M. Minaguti, E. Feitosa, T. C. V. Penna and A. Pessoa, *Sep. Purif. Technol.*, 2008, **62**, 166–174.
22 R. Hatti-Kaul, *Mol. Biotechnol.*, 2001, **19**, 269–278.
23 Y. K. Yau, C. W. Ooi, E.-P. Ng, J. C.-W. Lan, T. C. Ling and P. L. Show, *Bioresour. Bioprocess.*, 2015, **2**, 49.
24 N. Mekaoui, K. Faure and A. Berthod, *Bioanalysis*, 2012, **4**, 833–844.
25 M. T. Zafarani-Moattar and R. Sadeghi, *J. Chem. Eng. Data*, 2005, **50**, 947–950.
26 J. H. P. M. Santos, F. A. e Silva, J. A. P. Coutinho, S. P. M. Ventura and A. Pessoa, *Process Biochem.*, 2015, **50**, 661–668.
27 J. C. Merchuk, B. a Andrews and J. a. Asenjo, *J. Chromatogr. B: Biomed. Sci. Appl.*, 1998, **711**, 285–293.
28 G. P. Meneguetti, J. H. P. M. Santos, K. M. T. Obreque, C. M. Vaz Barbosa, G. Monteiro, S. H. P. Farsky, A. M. De Oliveira, C. B. Angeli, G. Palmisano, S. P. M. Ventura, A. Pessoa-Junior and C. De Oliveira Rangel-Yagui, *PLoS One*, 2019, **14**, e0211951.
29 L. Santiago-Rodríguez, J. Méndez, G. M. Flores-Fernandez, M. Pagán, J. A. Rodríguez-Martínez, C. R. Cabrera and K. Griebenow, *J. Electroanal. Chem.*, 2011, **663**, 1–7.
30 N. H. Kim, M. S. Jeong, S. Y. Choi and J. H. Kang, *Bull. Korean Chem. Soc.*, 2004, **25**, 1889–1892.
31 S. Aldrich, *Enzymatic Assay of Lysozyme*, 2019, URL: https://www.sigmaaldrich.com/technical-documents/protocols/biology/enzymatic-assay-of-lysozyme.html (available 15/09/19).
32 C. Drainas and J. A. Pateman, *Biochem. Soc. Trans.*, 1977, **5**, 259–261.
33 T. Iwase, A. Tajima, S. Sugimoto, K. I. Okuda, I. Hironaka, Y. Kamata, K. Takada and Y. Mizunoe, *Sci. Rep.*, 2013, **3**, 3081.
34 A. M. Azevedo, A. G. Gomes, P. A. J. Rosa, I. F. Ferreira, A. M. M. O. Pisco and M. R. Aires-Barros, *Sep. Purif. Technol.*, 2009, **65**, 14–21.
35 Y.-T. Wu, D.-Q. Lin and Z.-Q. Zhu, *Fluid Phase Equilib.*, 1998, **147**, 25–43.
36 S. C. Silvério, A. Wegrzyn, E. Lladosa, O. Rodríguez and E. A. MacEdo, *J. Chem. Eng. Data*, 2012, **57**, 1203–1208.
37 C. Delgado, M. Malmsten and J. M. Van Alstine, *J. Chromatogr. B: Biomed. Sci. Appl.*, 1997, **692**, 263–272.
38 C. Delgado, F. Malik, B. Selisko, D. Fisher and G. E. Francis, *J. Biochem. Biophys. Methods*, 1994, **29**, 237–250.
39 M. Galindo-López and M. Rito-Palomares, *J. Chem. Technol. Biotechnol.*, 2013, **88**, 49–54.
40 T. Sookkumnerd and J. T. Hsu, *J. Liq. Chromatogr. Relat. Technol.*, 2000, **23**, 497–503.
41 N. Schaeffer, M. Gras, H. Passos, V. Mogilireddy, C. M. N. Mendonça, E. Pereira, E. Chainet, I. Billard, J. A. P. Coutinho and N. Papaiconomou, *ACS Sustainable Chem. Eng.*, 2019, **7**, 1769–1777.
42 A. M. Ferreira, H. Passos, A. Okafuji, A. P. M. Tavares, H. Ohno, M. G. Freire and J. A. P. Coutinho, *Green Chem.*, 2018, **20**, 1218–1223.
43 S. P. M. Ventura, V. C. Santos-Ebinuma, J. F. B. Pereira, M. F. S. Teixeira, A. Pessoa and J. A. P. Coutinho, *J. Ind. Microbiol. Biotechnol.*, 2013, **40**, 507–516.
44 K. Shameli, M. B. Ahmad, S. D. Jazayeri, S. Sedaghat, P. Shabanzadeh, H. Jahangirian, M. Mahdavi and Y. Abdollahi, *Int. J. Mol. Sci.*, 2012, **13**, 6639–6650.

45 J. Kong and S. Yu, *Acta Biochim. Biophys. Sin.*, 2007, **39**, 549–559.
46 A. Natalello, D. Ami, M. Collini, L. D'Alfonso, G. Chirico, G. Tonon, S. Scaramuzza, R. Schrepfer and S. M. Doglia, *PLoS One*, 2012, **7**, e42511.
47 J. O. Speare and T. S. Rush, *Biopolymers*, 2003, **72**, 193–204.
48 C. J. Fee and J. M. Van Alstine, *Chem. Eng. Sci.*, 2006, **61**, 934–939.